

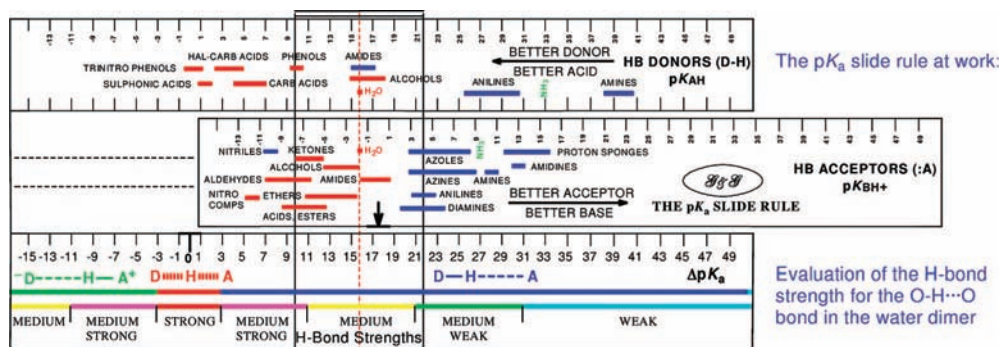
Predicting Hydrogen-Bond Strengths from Acid–Base Molecular Properties. The pK_a Slide Rule: Toward the Solution of a Long-Lasting Problem

PAOLA GILLI, LORETTA PRETTO, VALERIO BERTOLASI, AND GASTONE GILLI*

Dipartimento di Chimica and Centro di Strutturistica Diffraattometrica, Università di Ferrara, I-44100 Ferrara, Italy

RECEIVED ON JANUARY 1, 2008

CONSPECTUS



Unlike normal chemical bonds, hydrogen bonds (H-bonds) characteristically feature binding energies and contact distances that do not simply depend on the donor (D) and acceptor (:A) nature. Instead, their chemical context can lead to large variations even for a same donor–acceptor couple. As a striking example, the weak $\text{HO}-\text{H}\cdots\text{OH}_2$ bond in neutral water changes, in acidic or basic medium, to the 6-fold stronger and 15% shorter $[\text{H}_2\text{O}\cdots\text{H}\cdots\text{OH}_2]^+$ or $[\text{HO}\cdots\text{H}\cdots\text{OH}]^-$ bonds. This surprising behavior, sometimes called *the H-bond puzzle*, practically prevents prediction of H-bond strengths from the properties of the interacting molecules. Explaining this puzzle has been the main research interest of our laboratory in the last 20 years. Our first contribution was the proposal of RAHB (resonance-assisted H-bond), a new type of strong H-bond where donor and acceptor are linked by a short π -conjugated fragment. The RAHB discovery prompted new studies on strong H-bonds, finally leading to a general H-bond classification in six classes, called *the six chemical leitmotifs*, four of which include all known types of strong bonds. These studies attested to the covalent nature of the strong H-bond showing, by a formal valence-bond treatment, that weak H-bonds are basically electrostatic while stronger ones are mixtures of electrostatic and covalent contributions. The covalent component gradually increases as the difference of donor–acceptor proton affinities, ΔPA , or acidic constants, ΔpK_a , approaches zero. At this limit, the strong and symmetrical $\text{D}\cdots\text{H}\cdots\text{A}$ bonds formed can be viewed as true three-center-four-electron covalent bonds.

These results emphasize the role PA/pK_a equalization plays in strengthening the H-bond, a hypothesis often invoked in the past but never fully verified. In this Account, this hypothesis is reconsidered by using a new instrument, *the pKa slide rule*, a bar chart that reports in separate scales the pK_a 's of the D–H proton donors and :A proton acceptors most frequently involved in $\text{D}-\text{H}\cdots\text{A}$ bond formation. Allowing the two scales to shift so to bring selected donor and acceptor molecules into coincidence, the ruler permits graphical evaluation of ΔpK_a and then empirical appreciation of the $\text{D}-\text{H}\cdots\text{A}$ bond strength according to the pK_a equalization principle. Reliability of pK_a slide rule predictions has been verified by extensive comparison with two classical sources of H-bond strengths: (i) the gas-phase dissociation enthalpies of charged $[\text{X}\cdots\text{H}\cdots\text{X}]^-$ and $[\text{X}\cdots\text{H}\cdots\text{X}]^+$ bonds derived from the thermodynamic NIST Database and (ii) the geometries of more than 9500 H-bonds retrieved from the Cambridge Structural Database. The results attest that the pK_a slide rule provides a reliable solution for the long-standing problem of H-bond-strength prediction and represents an efficient and practical tool for making such predictions directly accessible to all scientists.

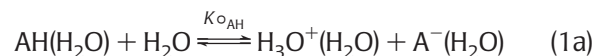
Introduction

The principle of PA/ pK_a equalization (or PA/ pK_a matching) is the hypothesis that the driving force of H-bond strengthening is to be identified in the progressive reduction of the difference of proton affinities, $\Delta PA = PA(D^-) - PA(A)$, or acidic constants, $\Delta pK_a = pK_{AH}(D-H) - pK_{BH^+}(A-H^+)$, of the donor and acceptor groups. This idea is not new, having been invoked in many older thermodynamic^{1–4} or spectroscopic^{5–7} studies and more recently revived in view of its possible applications to the rational design of molecular cocrystals⁸ and in connection with the ongoing controversy on the role it may play in enzymatic catalysis,^{9–17} though no generalization to the whole of H-bonds has been so far achieved. We have successfully applied such an empirical equalization rule to the analysis of chemical leitmotifs (CLs), the six classes in which all H-bonds can be partitioned,^{18–26} and a further verification has come from the recent treatment^{27–29} of the H-bond as a proton-transfer (PT) chemical reaction $D-H \cdots A \rightleftharpoons D \cdots H \cdots A \rightleftharpoons D \cdots H-A$ whose potential energy profile changes according to the PA/ pK_a difference between the donor and acceptor groups. This model, called transition-state H-bond theory (TSHBT), was applied to the DFT-simulated PT pathways of the tautomeric ketohydrazone–azoenol system yielding a substantial support of the assumptions done in terms of classical kinetic tools, such as Leffler–Hammond postulate, Marcus treatment, and LFER correlations.

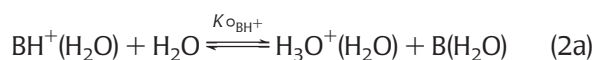
Now, it is clear that we could go on to study ever new particular cases obtaining ever new partial verifications of the same PA/ pK_a equalization principle. New more general methods are needed, to be applied with confidence to all H-bonds normally occurring in most chemical and biochemical systems. Accordingly, this paper is intended to develop a practical tool for predicting H-bond strengths from the acid–base parameters of the interacting molecules and to verify these predictions by comparing them with some comprehensive and reliable sources of experimental strengths. A choice between PA and pK_a was required and pK_a values in water^{30–34} were chosen as suitable acid–base indicators, while H-bond geometries from crystallographic databases^{35,36} and gas-phase bond dissociation enthalpies from the thermodynamic NIST Database^{37,38} were used as principal sources of bond-strength estimates. The reasons supporting these choices are detailed in a recent thermodynamic analysis of the problem, which has shown that ΔpK_a values can be computed for more H-bond classes than the ΔPA ones.³⁹

Definitions and Methods

pK_a Definitions. H-bond donors (D–H) are acids (A–H) with dissociation constant $K_a = K_{AH}^\circ$, and H-bond acceptors (:A) are bases (B) with dissociation constant $K_a = K_{BH^+}^\circ$, according to



$$\begin{aligned} \Delta_{AH}G^\circ &= -RT \ln K_{AH}^\circ = \Delta_{AH}H^\circ - T\Delta_{AH}S^\circ \\ &= 2.303RT pK_{AH} = 1.364 pK_{AH} \\ &(\text{kcal mol}^{-1} \text{ at } 25^\circ \text{C}) \end{aligned} \quad (1b)$$



$$\begin{aligned} \Delta_{BH^+}G^\circ &= -RT \ln K_{BH^+}^\circ = \Delta_{BH^+}H^\circ - T\Delta_{BH^+}S^\circ \\ &= 2.303RT pK_{BH^+} = 1.364 pK_{BH^+} \\ &(\text{kcal mol}^{-1} \text{ at } 25^\circ \text{C}) \end{aligned} \quad (2b)$$

The ΔpK_a associated with any D–H \cdots :A bond takes the form

$$\Delta pK_a(D-H \cdots :A) = pK_{AH}(D-H) - pK_{BH^+}(A-H^+) \quad (3)$$

and is negative or positive according to whether or not the $D \cdots H-A^+$ proton transfer occurred.

These definitions refer to the pK_a scale in water and have exact meaning only within its autoprotolysis range ($0 \leq pK_a \leq 14$). This range can be extended by using solvents more acidic or more basic than water, though the pK_a 's measured become less accurate the farther from the water range they are.^{30,31} The expansion is needed, however, to cover the exceedingly wide pK_a range of common H-bond donors and acceptors ($-14 \leq pK_a \leq 53$). Values were taken from previous compilations^{31–34} and arranged for chemical functionality in Tables S1 and S2 of the Supporting Information.

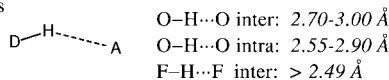
H-Bond Definitions. The H-bond is a D–H \cdots :A interaction between a proton donor D (an electronegative atom) and a proton acceptor or lone-pair carrier :A (another electronegative atom or a multiple π -bond).^{40,41} Availability of pK_a values determines the choice of donors (C, N, O, S, and halogens) and acceptors (N, P, O, S, and Se) that can be treated. Since the pK_a 's of π -bond acceptors are unknown, D–H $\cdots\pi$ -bonds are neglected.

The convention is adopted that, in any acid–base D–H \cdots :A bond, the donor is a neutral acid D–H (and not a protonated A–H⁺ cation) and the acceptor a neutral base :A (and not a deprotonated :D[−] anion). Therefore, both R–COO–H \cdots :NR₃ and R–COO[−] \cdots H–N⁺R₃ bonds are considered to derive from R–COO–H (an acid) and :NR₃ (a base),

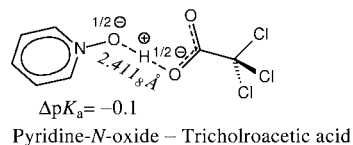
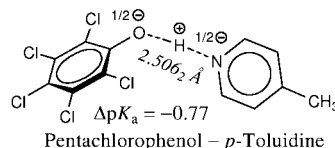
CHART 1

The Six H-Bond Chemical Leitmotifs (CLs)

NON-ASSISTED H-BONDS

CL # 1. OHB \Rightarrow Weak H-BondsOrdinary H-Bond
No PA/pK_a Matching $R-D-H \cdots A$ 

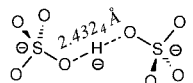
CHARGE-ASSISTED H-BONDS

CL # 2. (+/-)CAHB \Rightarrow Strong H-BondsDouble Charge-Assisted H-Bond
Direct Acid-Base PA/pK_a Matching $R-^{1/2-}D \cdots H^+ \cdots A^{1/2-}R$ 

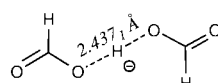
2.26-2.28 Å

F...H...F

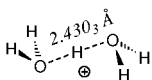
Hydrogen difluoride



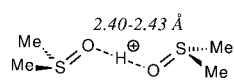
Hydrogen bis(sulfate)



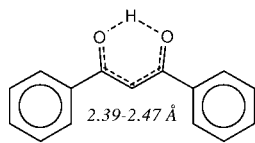
Hydrogen diformate

CL # 3. (-)CAHB \Rightarrow Strong H-BondsNegative Charge-Assisted H-Bond
Acid-Base PA/pK_a Matching by Proton Loss $[R-D \cdots H \cdots D-R]^-$ CL # 4. (+)CAHB \Rightarrow Strong H-BondsPositive Charge-Assisted H-Bond
Acid-Base PA/pK_a Matching by Proton Gain $[R-A \cdots H \cdots A-R]^+$ 

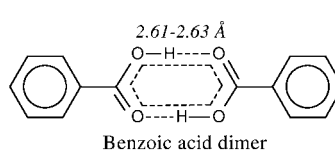
Hydron-bis(water)



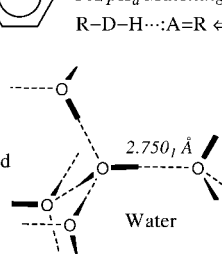
Hydron-bis(dimethyl-sulfoxide)

 Σ/Π -BOND POLARIZATION-ASSISTED H-BONDS

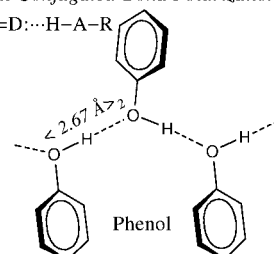
Dibenzoylmethane enols



Benzoic acid dimer

CL # 5. RAHB \Rightarrow Strong H-BondsResonance-Assisted or π -Bond Cooperative H-Bond
 PA/pK_a Matching by π -Conjugated-Bond Polarization $R-D-H \cdots A=R \Leftrightarrow R=D \cdots H-A-R$ 

Water



Phenol

CL # 6. PAHB \Rightarrow Medium-Strong H-BondsPolarization-Assisted or σ -Bond Cooperative H-Bond
(Partial) PA/pK_a Matching by σ -Bond Polarization $\cdots D-H \cdots D-H \cdots D-H \cdots$

whether or not the proton transfer occurred. In this way, proton-transfer information remains included in the sign of ΔpK_a .

Chemical Leitmotif Definitions. H-bonds are named after the classification in chemical leitmotifs (CLs),¹⁸⁻²¹ which are illustrated in Chart 1 by some significant examples and can be described as follows:

CL#1. OHB or *ordinary H-bond*, including normal $D-H \cdots A$ bonds which are neither charge- nor resonance-assisted and, for this reason, are weak, dissymmetric, and electrostatic in nature; they encompass, by far, the largest number of H-bonds.

CL#2. (\pm)CAHB or *double charge-assisted H-bond*, including strong $^{1/2-}D \cdots H^+ \cdots A^{1/2-}$ bonds deriving from the acid-base $D-H \cdots A \rightleftharpoons D: \cdots H-A^+$ equilibrium in conditions of close donor-acceptor pK_a matching.

CL#3. (-)CAHB or *negative charge-assisted H-bond*, including strong $[D \cdots H \cdots D]^-$ bonds deriving from the association of an acid with its conjugated base (such as $[R-COO \cdots H \cdots OOC-R]^-$ hydrogen dicarboxylates).

CL#4. (+)CAHB or *positive charge-assisted H-bond*, including strong $[A: \cdots H \cdots A]^+$ bonds formed by two bases capturing a proton (such as the $[H_2O \cdots H \cdots OH_2]^+$ ion).

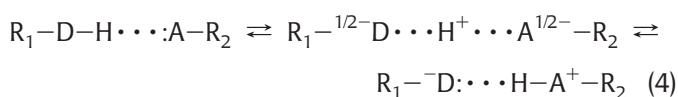
CL#5. R_n -RAHB or *resonance-assisted H-bond*,²²⁻²⁶ occurring when the donor (acid) and the acceptor (base) are connected by a short π -conjugated R_n fragment of n atoms (typically, R_3 -RAHBs include the strong $O-H \cdots O$ bonds formed by $\cdots O=C-C=C-OH \cdots$ β -diketone enols and R_1 -RAHBs the dimers or chains of carboxylic acids).

CL#6. PAHB or *polarization-assisted H-bond*, first proposed by Jeffrey⁴² with the name *σ -bond cooperative H-bond* to represent the class of moderate H-bonds associated with chains of $\cdots O-H \cdots O-H \cdots$ hydroxyl groups occurring, for example, in water and in alcohol and phenol crystals. Because σ -bonds are only weakly polarizable, these bonds are not much stronger than ordinary ones and, for the aims of this paper, can be associated with them.

This classification is important because practically all leitmotifs entertain different relationships with the pK_a equalization principle.³⁹ In fact,

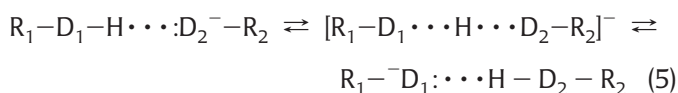
(i) RAHBs cannot be treated by pK_a equalization methods because of the impossibility of computing their ΔpK_a values. This is because RAHB formation affects the π -delocalization of the resonant fragment (e.g., $O=C-C=C-OH$ becomes $\cdots O\cdots C\cdots C\cdots C\cdots OH\cdots$) with consequent large perturbations of the pK_a 's of the two interacting moieties (in this example, the $C=C-OH$ enol and $C=O$ carbonyl groups)

(ii) Only OHBs and (\pm)CAHBs are associated with a true *proton transfer equilibrium*

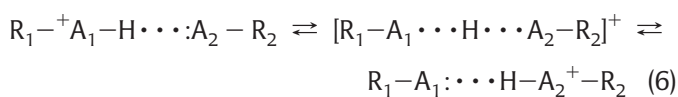


whose properties can be easily related to the acid–base difference $\Delta pK_a = pK_{AH}(R_1-D-H) - pK_{BH^+}(R_2-A-H^+)$

(iii) The other two CAHBs are more properly classified as *proton sharing equilibria* because ($-$)CAHBs derive from the sharing of a proton between two H-bond donors (two acids)



and ($+$)CAHBs from the proton sharing between two H-bond acceptors (two bases)



whose ΔpK_a becomes the pK_a difference of two acids [$\Delta pK_a = pK_{AH}(R_2-D_2-H) - pK_{AH}(R_1-D_1-H)$] or two bases [$\Delta pK_a = pK_{BH^+}(R_2-A_2-H^+) - pK_{BH^+}(R_1-A_1-H^+)$], respectively.

This leads to an important consequence: whenever the H-bond is both homonuclear ($D_1 = D_2$ or $A_1 = A_2$) and homomolecular ($R_1 = R_2$) *the matching condition $\Delta pK_a = 0$ will hold irrespective of the actual pK_a 's of the two interacting moieties*. This makes these complexes ideal for the study of strong H-bonds also because, being charged, they are the only ones for which gas-phase dissociation enthalpies can be measured.^{3,4,37,38}

Crystal and Energy Data. Crystal data were retrieved from crystallographic databases.^{35,36} For each $D-H\cdots A$ bond, values of $d_{D\cdots A}$, d_{D-H} , and $d_{H\cdots A}$ distances and $D-H-A$ angles were registered. H-bond strengths were estimated from $D\cdots A$ distances corrected for the $D-H-A$ angle to account for the energy decrease caused by linearity loss.^{43,44} Two strat-

egies were applied. In Table 1, where the search was limited to strong and mostly linear H-bonds, the simple $d_{D\cdots A}$ values were used within the limit $D-H-A > 160^\circ$. For Figure 4, where H-bonds of any strength were compared, the quantity $d'_{D\cdots A} = d_{D-H} + d_{H\cdots A}$ was computed, which naturally accounts for the angle and reduces to $d_{D\cdots A}$ when $D-H-A = 180^\circ$. Lists of crystal structures and histograms of H-bond geometries are given as Tables S3–S4 of the Supporting Information. Gas-phase dissociation enthalpies, E_{HB} 's, for homomolecular $[X\cdots H\cdots X]^-$ and $[X\cdots H\cdots X]^+$ complexes are taken from the NIST Database.^{37,38}

Results and Discussion

Description of the pK_a Slide Rule. The pK_a 's retrieved are ordered for chemical class in the bar chart of Figure 1 (called hereafter the *pK_a slide rule*). Data are arranged in two columns $D-H$ donors (or $A-H$ acids) on the right and $:A$ acceptors (or B bases) on the left, different colors indicating the atoms involved: green and red for inorganic hydracids and oxyacids, black for $C-H$ acids, blue, cyan, red, and magenta for N, P, O and S atoms, respectively. Figure 1 is in a form particularly suited for comparing the pK_a values of the most common H-bond donors and acceptors (as done below) but can be easily redrawn as a true slide rule by allowing the donor and acceptor scales to shift reciprocally so to bring into coincidence the donor and acceptor molecules. This is shown in the figure of the Conspectus, where the slide rule is set in such a way to permit graphical ΔpK_a evaluation and empirical strength appreciation for the $O-H\cdots O$ bond in the water dimer.

$C-H$ acids display the greatest spreading of values, $-11 \leq pK_a \leq 53$, practically covering the full range of H-bond phenomena. $C-H\cdots A$ bonds are not treated here because they have already been considered by Pedireddi and Desiraju⁴⁵ in a wide correlation between pK_a values (in DMSO) and $C-H\cdots O$ bond lengths of 551 CSD³⁵ crystal structures. Though these bonds are considerably weaker than conventional $O-H\cdots A$ or $N-H\cdots A$ ones, the role played by the pK_a matching is very similar, as confirmed by the structure of the $C-H\cdots O$ adduct of trinitromethane ($pK_a = 0.0$) with dioxane ($pK_a = 2.1$), reporting the shortest $C\cdots O$ distance (2.936 Å) ever observed.⁴⁶

Organic H-bond donors lie in the interval $-1 \leq pK_a \leq 40$, the strongest acids being trinitrophenols ($-0.7 \leq pK_a \leq 0.33$) and the weakest ones organic amines (pK_a around 39). The order of decreasing acidity is carboxylic acids > phenols > alcohols and amides > anilines > amines, and in each class of compounds, acidity is enhanced by halogenation or nitration. Thioles ($6.5 \leq pK_a \leq 11$), enols ($8.5 \leq pK_a \leq 12$), and

TABLE 1. Comparison of D···A Contact Distances ($d_{D···A}$ in Å) and H-Bond Energies (E_{HB} in kcal mol⁻¹) in CAHBs (Charge-Assisted H-Bonds) with Those in OHBs (Ordinary H-Bonds)^a

D—H···A	χ_P	$d_{D···A}(vdW)$	(OHB,min)			(CAHB,min)			(CAHB,mean)	
			$d_{D···A}$	SHR%	E_{HB}	$d_{D···A}$	SHR%	E_{HB}	$d_{D···A}$	n
[F···H···F] ⁻	3.98	3.59	2.49	-31	≤6	2.207	-38	42(3)	2.27(3)	17
[O···H···O] ⁻	3.44	3.70	2.70	-27	≤5	2.402	-35	27(1)	2.45(2)	225
[Cl···H···Cl] ⁻	3.16	4.22	3.69	-13	≤2	3.093	-30	24(3)	3.13(3)	15
[N···H···N] ⁻	3.04	3.76	3.05	-19	≤3	2.669	-29	12(-)	2.72(3)	7
[Br···H···Br] ⁻	2.96	4.46	3.91	-12	≤2	3.377	-24	19(3)		1
[S···H···S] ⁻	2.58	4.24	4.00	-6	≤1	3.454	-18	13(1)		1
[F···H···F] ⁺	3.98	3.59	2.49	-31	≤6	2.284	-36	25(2)	2.292(3)	2
[O···H···O] ⁺	3.44	3.70	2.70	-27	≤5	2.360	-36	32(2)	2.42(2)	91
[N···H···N] ⁺	3.04	3.76	3.05	-19	≤3	2.592	-31	26(2)	2.70(5)	85
[O···H···O] [±]	3.44	3.70	2.70	-27	≤5	2.381	-36	28.7		141
[N···H···O] [±]	(3.24)	3.73	2.87	-23	≤4	2.506	-33	(15.2)		305
[N···H···N] [±]	3.04	3.76	3.05	-19	≤3	2.682	-29	16.4		27

^a χ_P = Pauling's electronegativity; $d_{D···A}(vdW)$ = van der Waals D···A distance without H-bond; $d_{D···A}(OHB,min)$ and $d_{D···A}(CAHB,min)$ = minimum D···A distances observed in OHBs and CAHBs, respectively; $d_{D···A}(CAHB,mean)$ = average D···A distances for the current samples of n elements (samples deposited as Tables S3.1–12, Supporting Information); SHR% = percent $d_{D···A}$ shrinking with respect to $d_{D···A}(vdW)$; standard deviations in parentheses. E_{HB} 's for OHBs are averaged from a variety of traditional sources; E_{HB} 's for (-)CAHBs and (+)CAHBs are the gas-phase dissociation enthalpies of the homomolecular complexes [X···H···X]⁻ (X = F, Cl, Br), [HY···H···YH]⁻ (Y = O, S), [H₂N···H···NH₂]⁻, [HF···H···FH]⁺, [H₂O···H···OH₂]⁺ and [H₃N···H···NH₃]⁺ derived from the NIST Database,^{37,38} since gas-phase E_{HB} 's cannot be measured for (±)CAHBs, they have been interpolated by eq 7 (in italics) or calculated by the Lippincott and Schroeder method^{43,44} (in parentheses).

oximes ($10 \leq pK_a \leq 12$) are significantly more acidic than the corresponding alcohols ($15 \leq pK_a \leq 18$).

The pK_a range of organic H-bond acceptors ($-12 \leq pK_a \leq 16$) is shifted upward with respect to that of H-bond donors. In consequence, a large group of acceptors (nitro and carbonyl compounds, nitriles, ethers, alcohols, and sulfoxides) fall in a region facing a few inorganic acids but no organic donors and are then expected to form only rather weak H-bonds with the latter. The same happens for the weakest H-bond donors (amines, anilines, and alcohols), which do not face any known acceptor.

Maximum overlap between donors and acceptors occurs in the interval $0 \leq pK_a \leq 14$ (the same as the pK_a 's measurable in water) where the greatest number of strong H-bonds is therefore expected. In theory, these short bonds should occur for $\Delta pK_a = 0$. In practice, the pK_a matching does not need to be so perfect and a variety of data suggest that misfits of ± 2.5 pK_a units are still compatible with strong H-bond formation. There are indications, moreover, that the $\Delta pK_a(\text{critical})$ (the ΔpK_a for which the proton transfer amounts to 50%) is not always zero but may assume small negative values depending on the environment.^{6,39,47–49} This is because our predictions are based on the pK_a 's in water, a solvent of high dielectric constant, which stabilizes ionic against neutral H-bonds.¹ Sobczyk⁴⁹ has suggested that for diffraction experiments in the solid state, the $\Delta pK_a(\text{critical})$ is shifted by nearly -1.5 pK_a units. In interpreting crystal structures, we must then assume that proton transfer occurs only for $\Delta pK_a \leq -1.5$ and that the best interval of close pK_a matching has to be shifted to some $-4.0 \leq pK_a \leq 1.0$.

These few considerations indicate that the pK_a slide rule may have important applications in predicting the occurrence of strong H-bonds, which remain defined as the bonds formed by two molecular partners lying on a same horizontal line in the slide rule itself. This, of course, is just a hypothesis, which needs to be validated by accurate comparisons with the experimental findings, and this is what is done in the next sections.

Two Projects for Verifying the pK_a Equalization Principle. Full verification of the pK_a equalization principle is clearly impracticable in front of tens of thousands of H-bonded crystal structures and thousands of combining molecules with often unknown or uncertain pK_a values. We must fall back on smaller projects that, though retaining good diagnostic capabilities, can handle more limited sets of structures and circumvent the chronic lack of accurate pK_a values. Accordingly, we have selected two projects intended to show that (i) all strong (short) H-bonds have null or very small ΔpK_a values and (ii) in any selected D—H···A system (here the N—H···O/O—H···N one) H-bond strengths (lengths) are modulated by the ΔpK_a over the full ΔpK_a range.

First Project. All Strong (Short) H-Bonds Have Null or Very Small ΔpK_a Values. Homomolecular (-)CAHBs and (+)CAHBs, having $\Delta pK_a = 0$ by definition, as well as the (±)CAHBs endowed with very small ΔpK_a values, should give rise to remarkably shorter and more energetic H-bonds than OHBs, which are normally associated with rather large ΔpK_a values (for instance, 21–25 and 14–19 pK_a units for the common alcohol–ketone and amide–amide couples). Table 1 collects the crystallographic and thermodynamic data needed to verify this hypothesis and Figure 2 displays some

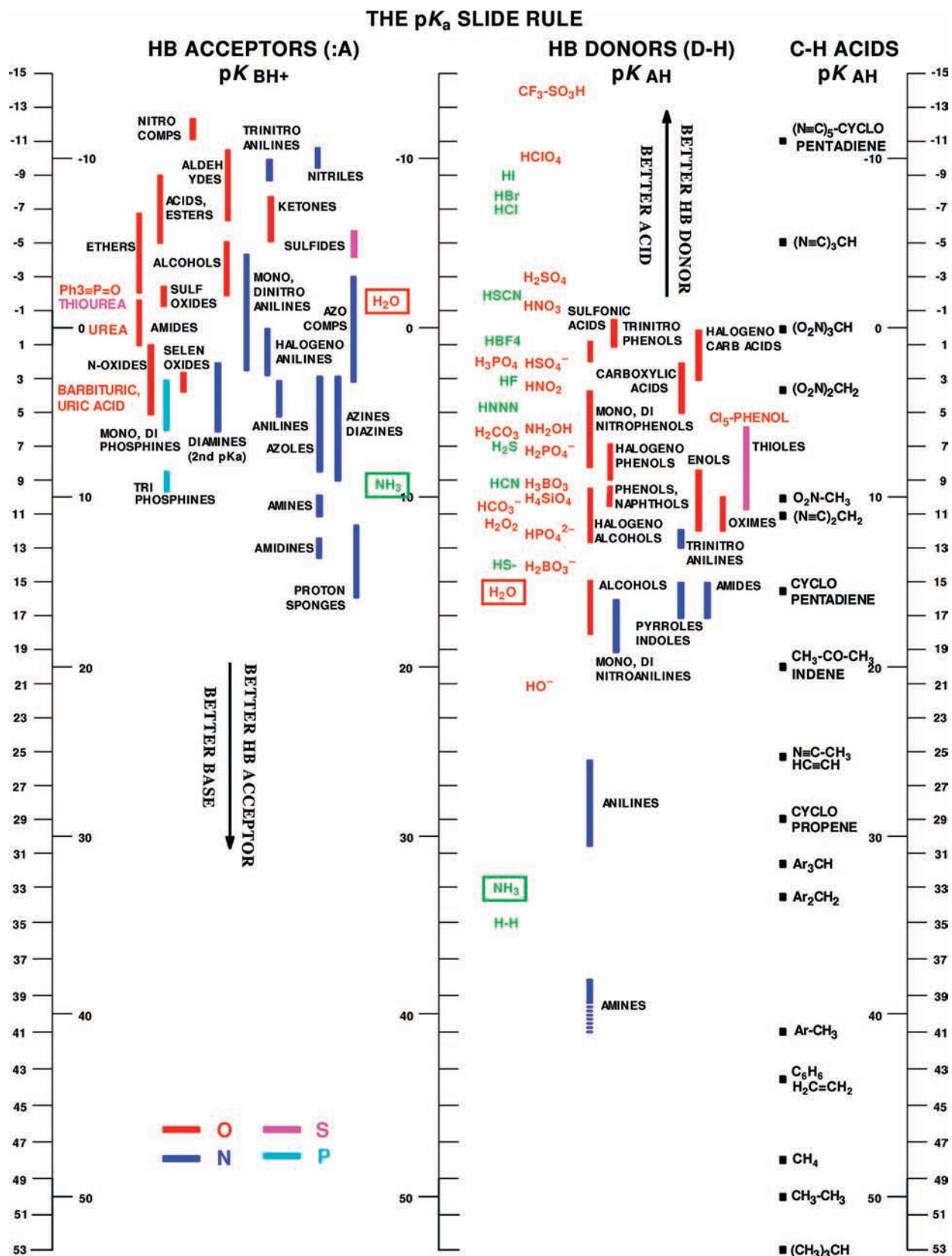


FIGURE 1. The pK_a slide rule. The figure represents, in the form of bar chart, the pK_a values of the most important classes of H-bond donors (right) and acceptors (left). Different colors indicate the atoms involved: green and red for inorganic hydric acids and oxyacids; black for C–H acids; blue, cyan, red, and magenta for N, P, O and S atoms, respectively. Strong H-bonds with strict pK_a matching are to be formed by two molecular partners that lie on a same horizontal line.

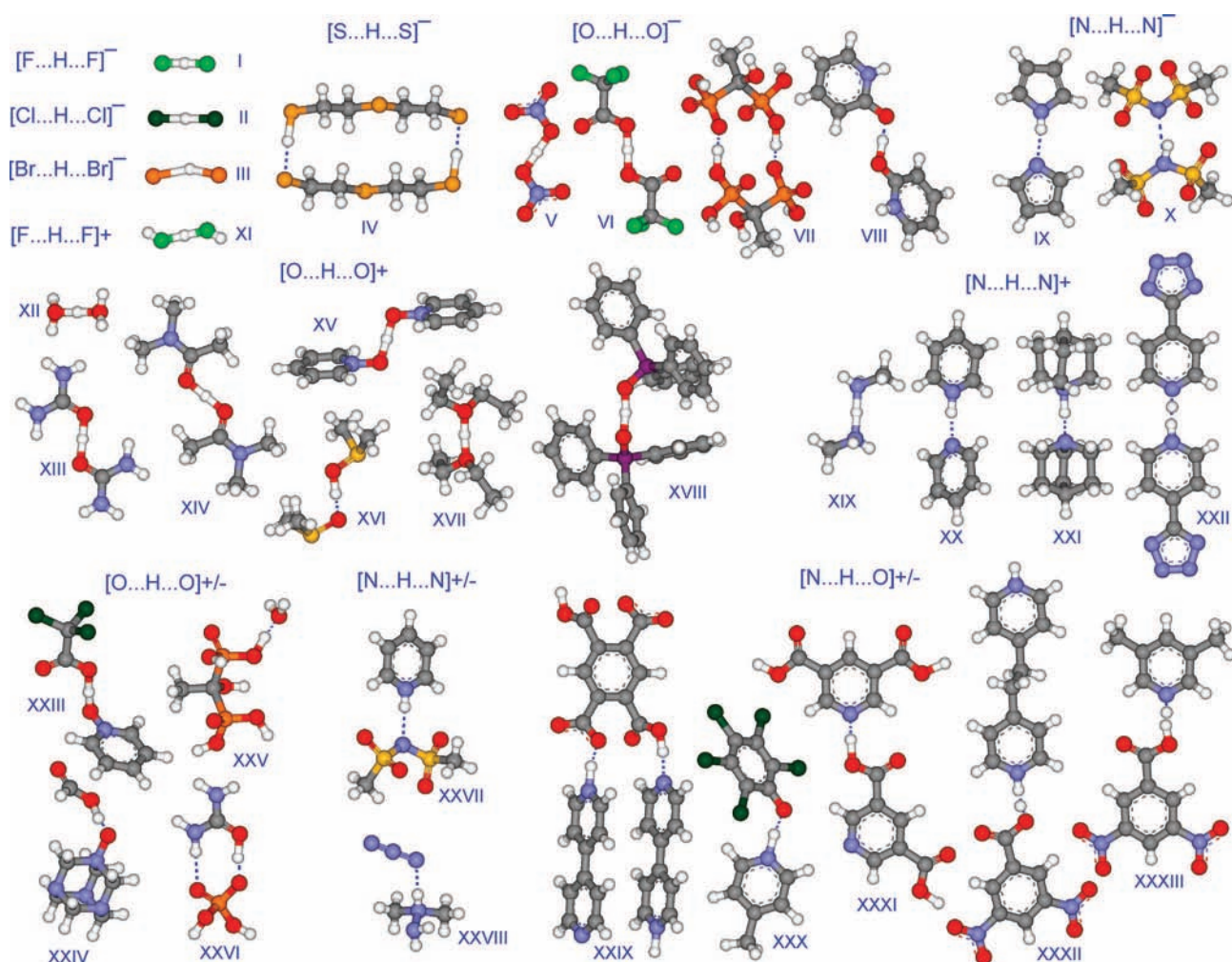


FIGURE 2. Some of the most characteristic examples of molecules forming strong homomolecular (–)CAHBs and (+)CAHBs with $\Delta pK_a = 0$, together with a number of (±)CAHBs selected for their small ΔpK_a values. Each structure is identified by the following string: CSD/ICSD Refcode, X-rays/neutron-temperature; $d_{D...A}$ (Å), ΔpK_a , $[D \cdots H \cdots A]^\pm$: (I) hydrogen difluoride (FEDDOH, X-295K; 2.238, 0.0); (II) hydrogen dichloride (CERVAW, X-295K; 3.108, 0.0); (III) hydrogen dibromide (KEGXUP, X-295K; 3.377, 0.0); (IV) 3-thiapentane-1-thiol-5-thiolate (YAJHEW, X-171K; 3.454, 0.0); (V) hydrogen dinitrate (AFUZAC, X-295K; 2.439, 0.0); (VI) hydrogen bis(trifluoroacetate) (KHFLAC01, N-295K; 2.419, 0.0); (VII) trihydrogen 1-hydroxyethane-1,1-diphosphate (SATHIE01, N-295K; 2.433, 0.0); (VIII) hydrogen bis(pyridinium-2-hydroxylate) (GOHHOA, X-143K; 2.418, 0.0); (IX) hydrogen dipyrrolide (YAKXIS, X-153K; 2.697, 0.0); (X) hydrogen bis(bis(methylsulfonyl) amidate) (RUJDAB, X-173K; 2.669, 0.0). $[A \cdots H \cdots A]^\pm$: (XI) fluoronium ion (71453-ICSD, X-295K; 2.284, 0.0); (XII) hydron-bis(water) (COLNUM01, N-20K; 2.430, 0.0); (XIII) hydron-bis(urea) (BADCIS10, X-295K; 2.424, 0.0); (XIV) hydron-bis(*N,N*-dimethylacetamide) (HDMAAU01, N-295K; 2.432, 0.0); (XV) hydron-bis(pyridine-*N*-oxide) (BALGUQ10, X-295K; 2.410, 0.0); (XVI) hydron-bis(dimethylsulfoxide) (JIMKAR01, X-295K, 2.414, 0.0); (XVII) hydron-bis(diethylether) (DIDTIT, X-203K; 2.394, 0.0); (XVIII) hydron-bis(triphenylphosphineoxide) (TPOPHX01, X-153K; 2.416, 0.0); (XIX) hydron-bis(methylamine) (ROHTIR, X-200K; 2.620, 0.0); (XX) hydron-bis(pyridine) (PYDMPS, X-295K; 2.656, 0.0); (XXI) hydron-bis(quinuclidine) (YERLOW, X-200K; 2.637, 0.0); (XXII) hydron-bis(4-tetrazolopyridine) (AYADOT, X-90K; 2.631, 0.0). $[D \cdots H \cdots A]^\pm$: (XXIII) pyridine-*N*-oxide-trichloroacetic acid (PYOTCA01, N-120K; 2.430, –1.3); (XXIV) HMTA-*N*-oxide-formic acid (HMTFA07, N-123K; 2.428, –0.9); (XXV) 1,1-hydroxyethane-1,1-diphosphoric acid–water (ETHDPH01, N-293K; 2.437, 3.3); (XXVI) urea–phosphoric acid (CRBAMP01, N-100K; 2.409, 2.1); (XXVII) pyridine–bis(methylsulfonyl)amide (QUSLEV, X-143K; 2.797, –2.4); (XXVIII) 1,1-dimethylhydrazine–hydrazoic acid (CORRUW, X-173K; 2.762, –3.4); (XXIX) 4,4'-bipyridine–benzene-1,2,4,5-tetracarboxylic acid (WISNAN01, N-20K; 2.522, –1.6); (XXX) 4-methylpyridine–pentachlorophenol (RAKQAV, N-20K; 2.506, –0.7); (XXXI) dinicotinic acid (DINICA11, N-15K; 2.523, 1.0); (XXXII) 1,2-dipyrid-4-ylethane–3,5-dinitrobenzoic acid (QIBSOJ, X-150K; 2.521, –2.2); (XXXIII) 3,5-dimethylpyridine–3,5-dinitrobenzoic acid (PUHROZ, X-80K; 2.529, –3.4).

of the most characteristic examples of molecules forming such strong charge-assisted H-bonds.

Data of Table 1 show that the transition from OHB to (–)CAHB or (+)CAHB (that is, from large to null ΔpK_a) causes

an important shortening of the $D \cdots A$ distances together with a much more important increase of the H-bond energies, so confirming the validity of the pK_a equalization principle and the reliability of the pK_a slide rule as a tool for H-bond anal-

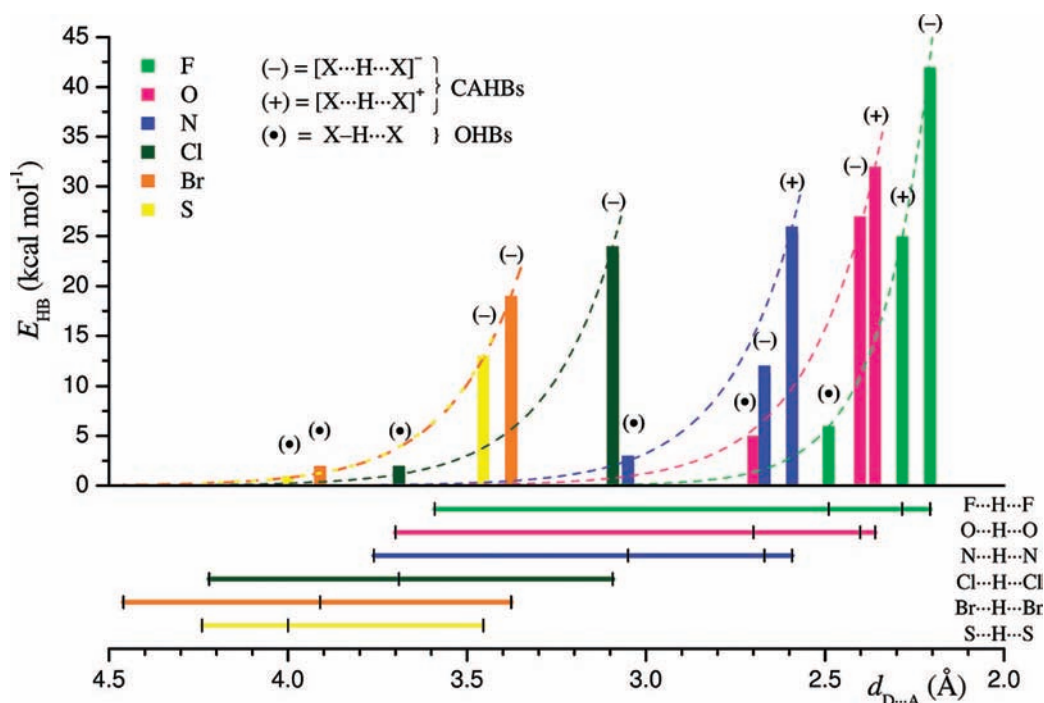


FIGURE 3. Full range of H-bond energies and $D \cdots A$ distances spanned by the most common homonuclear H-bonds, which do or do not fulfill the pK_a equalization condition (CAHBs and OHBs, respectively) based on data from Table 1. E_{HB} bond energies (in kcal mol^{-1}) of OHBs, marked as (\bullet) , and CAHBs, marked as $(-)$ or $(+)$, are reported as colored vertical bars occurring at their proper $D \cdots A$ distances (in \AA); colored horizontal lines on the bottom show the full ranges of variation of the $D \cdots A$ distances for each type of bond from $d_{D \cdots A}(\text{vdW})$ to the shortest value $d_{D \cdots A, \text{min}}$ having $E_{HB} = E_{HB, \text{MAX}}$. The dashed curves represent the exponential dependence of E_{HB} on $d_{D \cdots A}$ according to eq 7 with $k = 5.1$ for all bonds except $F \cdots H \cdots F$, for which $k = 7.0$.

ysis. These data are better illustrated in the form of a bar chart (Figure 3), where E_{HB} bond energies of OHBs, marked as (\bullet) , and CAHBs, marked as $(-)$ or $(+)$, are reported as colored vertical bars at their proper $D \cdots A$ distances, whose full range of variation is indicated by the colored horizontal lines on the bottom. Energies increase steeply with the $D \cdots A$ shrinking, and the functional form of this dependence can be modeled according to Lippincott and Schroeder's treatment of the linear $O-H \cdots O$ bond.^{43,44} Here, energies and distances are found to be linked by the regression equation

$$E_{HB} = E_{HB, \text{MAX}} \exp[-k(d_{D \cdots A} - d_{D \cdots A, \text{min}})] \quad (7)$$

where $E_{HB, \text{MAX}}$ is the highest energy associated with the minimum $d_{D \cdots A, \text{min}}$ distance and k is a least-squares constant. This equation fits reasonably well all data of Table 1 (dashed curves of Figure 3) providing a unified insight into the relationships between energies and distances in the H-bonds treated and allowing interpolation of the energies of bonds for which linear $D \cdots A$ distances are available but gas-phase energies cannot be measured (typically OHBs and (\pm) CAHBs). By this method, energies around 28.7 and 16.4 kcal mol^{-1} (in italics in Table 1) are calculated for the shortest $[O \cdots H \cdots O]^{\pm}$ and $[N \cdots H \cdots N]^{\pm}$ bonds.

Second Project. $N-H \cdots O/O-H \cdots N$ Bond Strengths (Lengths) Are Modulated by the ΔpK_a over the Full ΔpK_a Range. The ΔpK_a range where the H-bond is defined is enormous, $-30 \leq \Delta pK_a \leq 65$, when evaluated from the pK_a slide rule of Figure 1. Having already verified that the pK_a equalization principle holds in the restricted interval around zero, the problem is now whether and how such a rule can be extended to the full ΔpK_a range.

Verification of this hypothesis has been accomplished through a CSD³⁵ analysis of the $N-H \cdots O/O-H \cdots N$ bond, a system chosen for its outstanding chemical and biological importance. First, functional groups more frequently involved in these interactions were identified. Next, 10 classes of donors and 11 of acceptors were selected, and the search was restarted for each separate donor-acceptor couple. Altogether, 8681 bonds were analyzed (3968 $N-H \cdots O$, 2295 $O-H \cdots N$, and 2418 $^+N-H \cdots O^-$). $N \cdots O$ distances were evaluated as $d'_{N \cdots O} = d_{N-H} + d_{H-O}$ to account for the variability of the $N-H-O$ angle, and for each group, the minimum and average distances [$d_{N \cdots O}(\text{min})$ and $d_{N \cdots O}(\text{mean})$] were registered.⁵⁰ These values are compared in Figure 4 with the acid-base features of the donors (pK_{AH} range), acceptors (pK_{BH^+} range), and their combinations (ΔpK_a range). Each box is divided in two parts to account for neutral ($N-H \cdots O$

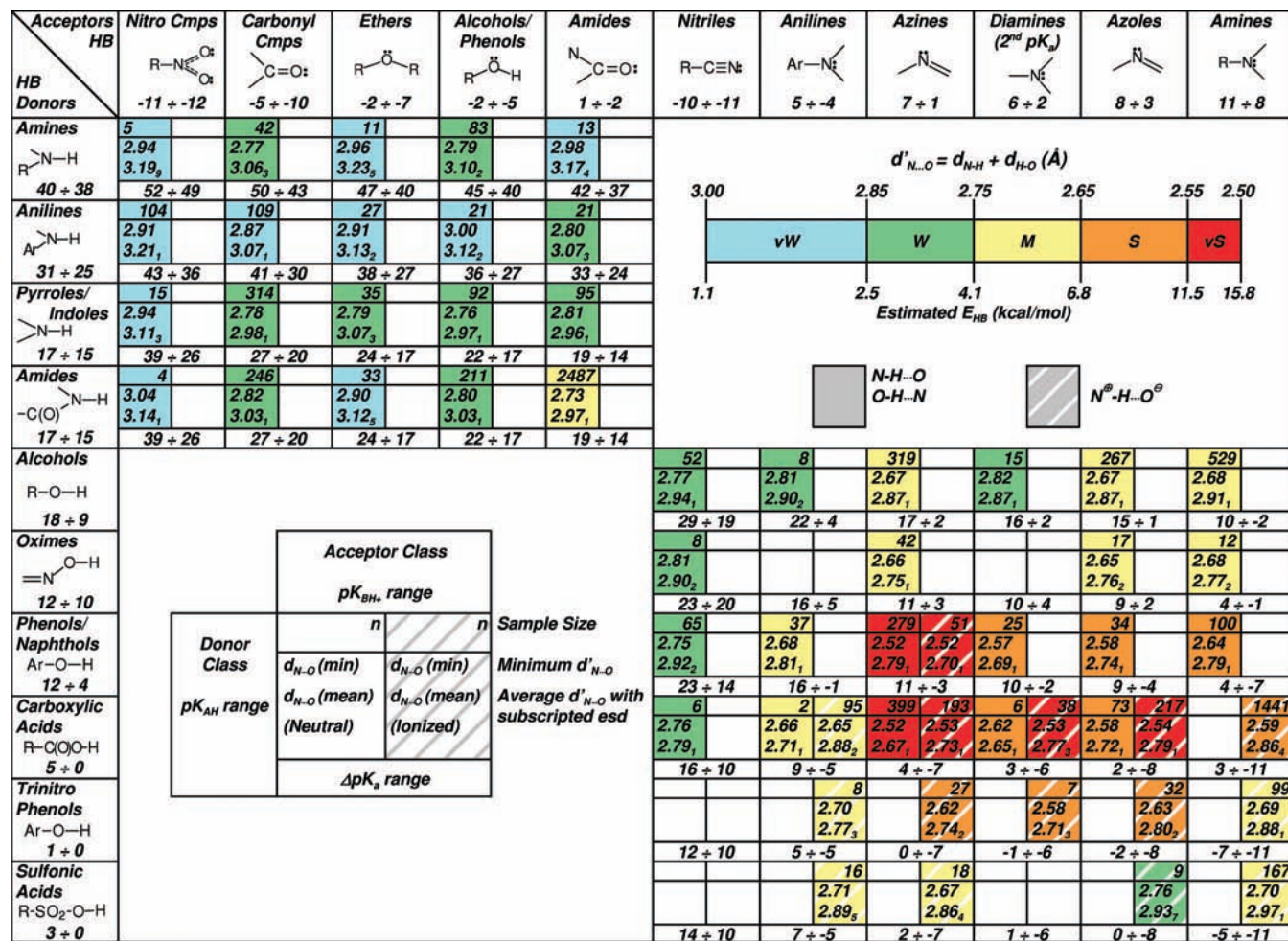


FIGURE 4. Minimum and average N...O distances [$d_{N...O}(\text{min})$ and $d_{N...O}(\text{mean})$, in Å] obtained from a CSD³⁵ search of the N-H...O/O-H...N bonds formed between common O-H and N-H donors and :O and :N acceptors. $d_{N...O}$ is calculated as $d'_{N...O} = d_{N-H} + d_{H-O}$ to account for the variability of the N-H-O angle. Bond lengths are divided in the five color-coded groups shown in the right top of the figure together with the corresponding H-bond energy values estimated by the Lippincott and Schroeder method.^{43,44} Observed distances are compared with the acid-base properties of donors (pK_{AH} range) and acceptors (pK_{BH+} range) and of their combinations (ΔpK_a range). Each box is divided in two parts to account for neutral (N-H...O or O-H...N; on the left) or charged (⁺N-H...O⁻; dashed on the right) H-bonds.

or O-H...N; on the left) or charged (⁺N-H...O⁻; dashed on the right) H-bonds. Bond lengths are divided in the five color-coded groups shown in the right top of the figure together with the corresponding H-bond energies estimated by the Lippincott and Schroeder method.^{43,44} The information obtained is statistical because individual pK_a's are unknown and, accordingly, D...A distances can only be compared with the average ΔpK_a intervals of each donor-acceptor group. Notwithstanding, a number of regularities are observed supporting the idea that H-bond strengths are essentially ΔpK_a-driven in the complete range of ΔpK_a values.

All N-H...O bonds (upper left rectangle of Figure 4) are weak because the donors (amines and anilines) are exceedingly weak acids ($25 \leq \text{pK}_a \leq 40$) not facing acceptors of comparable acidity in the pK_a slide rule. Only pyrroles and amides start to be

acidic enough ($15 \leq \text{pK}_a \leq 17$) to make moderately strong bonds with less acidic protonated acceptors, such as amides themselves ($-2 \leq \text{pK}_a \leq 1$). The resulting amide-amide ΔpK_a range (19-14) remains, however, too far from zero to permit strong H-bond formation.

All strong H-bonds gather in the lower right rectangle of the figure because, here, the ΔpK_a domain ($-11 \leq \Delta\text{pK}_a \leq 29$) encompasses positive, zero, and negative values, so making it possible to produce weak O-H...N, strong ^{1/2}-N...H⁺...O^{1/2-}, and weak ⁺N-H...O⁻ bonds. Since donors and acceptors are plotted in decreasing and increasing pK_a order, respectively, the ΔpK_a intervals of the different classes decrease from positive to negative along the main diagonal of the rectangle, concentrating nearly zero values near the center. According to expectation, along the diagonal we move from weak O-H...N

alcohol–nitrile bonds ($\Delta pK_a = 29 - 19$; $d_{N...O}(\text{min}) = 2.77 \text{ \AA}$; $d_{N...O}(\text{mean}) = 2.94[1] \text{ \AA}$; $n = 52$) to equally weak $^+N-H \cdots O^-$ sulfonic acid–amine bonds ($\Delta pK_a = -5$ to -11 ; $d_{N...O}(\text{min}) = 2.70 \text{ \AA}$; $d_{N...O}(\text{mean}) = 2.97[1] \text{ \AA}$; $n = 167$), while the center is occupied by a block of bonds (marked in red) associated with the complexes of phenols and carboxylic acids with azines, azoles, and second aminic moieties of monoprotonated diamines, which are much stronger ($d_{N...O}(\text{min})$ down to 2.52 \AA) because their global ΔpK_a range of 11 to -8 encompasses the zero, and a consistent fraction of them is expected to fall within the interval of true pK_a matching.

A last property that appears to change with regularity along the main diagonal of Figure 4 is the ratio between ionized ($^+N-H \cdots O^-$) and neutral ($N-H \cdots O$ or $O-H \cdots N$) H-bonds. Out of the 56 donor–acceptor couples considered, only the 15 located in the lower right angle actually form ionized bonds, so showing that the $N-H \cdots O/O-H \cdots N$ system is strongly dissymmetric with respect to proton transfer. This dissymmetry is a general feature of the H-bond phenomenon and reflects an even more basic dissymmetry between proton donors, covering the full range of accessible pK_a values, and proton acceptors, which span less than one-half of it, as evident from the donor–acceptor misfit in the pK_a slide rule of Figure 1.

Summary and Conclusions

The pK_a equalization principle states that the strength of the $D-H \cdots A$ bond increases with decreasing $\Delta pK_a = pK_a(D-H) - pK_a(A-H^+)$, the difference of acidic constants of the H-bond donor and acceptor, and that such a strength reaches a maximum when ΔpK_a approaches zero. The principle has never been verified in its generality for lack of a congruous coverage of the full pK_a ladder of the H-bond partners.

By extensive bibliographic search, such a ladder has been built up as a comprehensive list of pK_a values reduced to water and found to span the impressive ranges of $-14 \leq pK_a \leq 53$ for donors and $-12 \leq pK_a \leq 16$ for acceptors. These data are now made available as deposited pK_a tables and in the form of the “ pK_a slide rule”, which is a bar chart reporting, in separate columns, the pK_a 's of the most common classes of $D-H$ donors and $:A$ acceptors (globally 103 entries) and permits approximate graphical evaluation of ΔpK_a for any donor–acceptor couple, so allowing empirical prediction of the H-bond strengths in terms of pK_a matching.

Extended comparison of these predictions with the H-bond strengths derived from crystal structure geometries and gas-phase dissociation enthalpies has led to substantiation of the pK_a equalization principle over the full range of ΔpK_a values ($-30 \leq \Delta pK_a \leq 65$) for all the H-bond chemical leitmotifs for which the

ΔpK_a can be computed. These accessible classes include all proton-transfer (acid–base) H-bonds [OHBs, PAHBs, and (\pm)CAHBs] and two out of three proton-sharing ones [($-$)CAHBs and ($+$)CAHBs], RAHBs remaining however excluded because of the practical impossibility of evaluating the proper value of ΔpK_a . All this suggests that ΔpK_a -based methods may play a prominent diagnostic role for approximate but quick evaluation of the strengths of the great majority of H-bonds, particularly if the pK_a slide rule will be completed, in the future, by inclusion of the many chemical groups for which acid–base constants are still missing.

Most of the concepts developed in this Account, in particular the PA/ pK_a equalization principle and the practical applications of the pK_a slide rule, will be reconsidered in a wider context in a forthcoming book⁵¹ on the nature of the H-bond.

This work was supported by COFIN-2004 (MIUR, Rome) and by the University of Ferrara with local research funds (FAR).

Supporting Information Available. pK_a lists used for compiling the bar chart of Figure 1; tables and histograms of H-bond geometries summarized in Table 1; CSD Refcodes of the 8681 crystal structures used as input for Figure 4. This material is available free of charge via the Internet at <http://pubs.acs.org>.

BIOGRAPHICAL INFORMATION

Paola Gilli obtained a degree in Chemistry in 1990 and a Ph.D. in Physical Chemistry in 1994 from the University of Ferrara. She has been a postdoctoral fellow at the Cambridge Crystallographic Data Centre (U.K.) directed by Olga Kennard and at the ICSN-CNRS Laboratoire de Cristallographie (Gif-sur-Yvette, France) directed by Claudine Pascard. Since 1997, she has been a Senior Researcher and Lecturer in Physical Chemistry at the University of Ferrara. Her main research interests are in the fields of molecular interactions, structural chemistry, applied quantum mechanics, and biothermodynamics, with emphasis on hydrogen bond phenomena.

Loretta Pretto obtained a degree in Chemistry in 2000 and a Ph.D. in Physical Chemistry in 2004 from the University of Ferrara. Her current research interests are in X-ray crystallography, structural databases, and molecular dynamics simulation of drug–receptor binding.

Valerio Bertolasi obtained a degree in Chemistry in 1973 and has been Associate Professor of Chemistry at the University of Ferrara since 1983. He has been postdoctoral fellow at the Laboratoire de Minéralogie-Cristallographie of the Université de Paris VI (France) under the supervision of Prof. J. P. Mornon. An expert of high-precision low-temperature X-ray crystallography of organic and organometallic compounds, he is author of over 250 papers mostly in the fields of crystal engineering, supramolecular chemistry, structural correlations, and solid-state tautomerism.

Gastone Gilli obtained a degree in Chemistry in 1961, has been Full Professor of Chemistry since 1975, and holds the Chair of Physical

Chemistry at the University of Ferrara, where he has acted as Director of the Centre of Structural Diffractometry since 1969. Trained in materials science, he moved to structural crystallography after a 1971 NATO Fellowship with Professor D.W.J. Cruickshank at UMIST (UK). Since then, he has devoted his activity to structural chemistry, structure–property relationships, molecular interaction theory, and thermodynamics of biological systems. He is a recognized expert in the field of hydrogen bonding and binding thermodynamics.

FOOTNOTES

*To whom correspondence should be addressed. Mailing address: Dipartimento di Chimica and Centro di Strutturistica Diffrattometrica, Università di Ferrara, Via L. Borsari, 46, 44100 Ferrara (Italy). E-mail: ggilli.chim@unife.it. Tel: +39-0532 455141. Fax: +39-0532 240709.

REFERENCES

- Huyskens, P. L.; Zeegers-Huyskens, Th. Molecular Associations and Acid-Base Equilibriums. *J. Chim. Phys. Phys.-Chim. Biol.* **1964**, *61*, 81–86.
- Zeegers-Huyskens, Th. Energies of Hydroxy···Halide Ion (OH···X⁻) Hydrogen Bonds in the Gas Phase and Proton Affinities. *Chem. Phys. Lett.* **1986**, *129*, 172–175.
- Kearle, P. Ion Thermochemistry and Solvation from Gas Phase Ion Equilibriums. *Annu. Rev. Phys. Chem.* **1977**, *28*, 445–476.
- Meot-Ner (Mautner), M. Ionic Hydrogen Bonds. Part I. Thermochemistry, Structural Implications, and Role in Ion Solvation. In *Molecular Structure and Energetics*; Liebman, J. F., Greenberg, A., Eds.; VCH: Weinheim, Germany, 1987; Vol. 4, Chapter 3, pp 71–103.
- Ault, B. S.; Steinback, E.; Pimentel, G. G. Matrix Isolation Studies of Hydrogen Bonding. Vibrational Correlation Diagram. *J. Phys. Chem.* **1975**, *79*, 615–620.
- Malarski, Z.; Rospenk, M.; Sobczyk, L. Dielectric and Spectroscopic Studies of Pentachlorophenol–Amine Complexes. *J. Phys. Chem.* **1982**, *86*, 401–406.
- Barnes, A. J. Molecular Complexes of the Hydrogen Halides Studied by Matrix Isolation Infrared Spectroscopy. *J. Mol. Struct.* **1983**, *100*, 259–280.
- Aakeröy, C. B.; Desper, J.; Urbina, J. F. Supramolecular Reagents: Versatile Tools for Non-Covalent Synthesis. *Chem. Commun.* **2005**, 2820–2822.
- Cleland, W. W.; Kreevoy, M. M. Low-Barrier Hydrogen Bonds and Enzymatic Catalysis. *Science* **1994**, *264*, 1887–1890.
- Frey, P. A.; Whitt, S. A.; Tobin, J. B. A Low-Barrier Hydrogen Bond in the Catalytic Triad of Serine Proteases. *Science* **1994**, *264*, 1927–1930.
- Frey, P. A. Strong Hydrogen Bonding in Molecules and Enzymatic Complexes. *Magn. Reson. Chem.* **2001**, *39*, S190–S198.
- Harris, T. K.; Mildvan, A. S. High-Precision Measurement of Hydrogen Bond Lengths in Proteins by Nuclear Magnetic Resonance Methods. *Proteins* **1999**, *35*, 275–282.
- Cavalli, A.; Carloni, P.; Recanatini, M. Target-Related Applications of First Principles Quantum Chemical Methods in Drug Design. *Chem. Rev.* **2006**, *106*, 3497–3519.
- Warshel, A.; Papazyan, A.; Kollman, P. A. On Low-Barrier Hydrogen Bonds and Enzyme Catalysis. *Science* **1995**, *269*, 102–103.
- Shan, S.-O.; Loh, S.; Herschlag, D. The Energetics of Hydrogen Bonds in Model Systems: Implications for Enzymatic Catalysis. *Science* **1996**, *272*, 97–101.
- Guthrie, J. P. Short Strong Hydrogen Bonds: Can They Explain Enzymatic Catalysis? *Chem. Biol.* **1996**, *3*, 163–170.
- Perrin, C. L.; Nielson, J. B. “Strong” Hydrogen Bonds in Chemistry and Biology. *Annu. Rev. Phys. Chem.* **1997**, *48*, 511–544.
- Gilli, P.; Bertolasi, V.; Ferretti, V.; Gilli, G. Evidence for Resonance-Assisted Hydrogen Bonding. 4. Covalent Nature of the Strong Homonuclear Hydrogen Bond. Study of the O–H···O System by Crystal Structure Correlation Methods. *J. Am. Chem. Soc.* **1994**, *116*, 909–915.
- Gilli, P.; Ferretti, V.; Bertolasi, V.; Gilli, G. A Novel Approach to Hydrogen Bonding Theory. In *Advances in Molecular Structure Research*; Hargittai, I., Hargittai, M., Eds.; JAI Press Inc.: Greenwich, CT, 1996, Vol. 2, pp 67–102.
- Gilli, G.; Gilli, P. Towards a Unified Hydrogen-Bond Theory. *J. Mol. Struct.* **2000**, *552*, 1–15.
- Gilli, P.; Bertolasi, V.; Pretto, L.; Ferretti, V.; Gilli, G. Covalent versus Electrostatic Nature of the Strong Hydrogen Bond: Discrimination among Single, Double, and Asymmetric Single-Well Hydrogen Bonds by Variable-Temperature X-Ray Crystallographic Methods in β -Diketone Enol RAHB Systems. *J. Am. Chem. Soc.* **2004**, *126*, 3845–3855.
- Gilli, G.; Bellucci, F.; Ferretti, V.; Bertolasi, V. Evidence for Resonance-Assisted Hydrogen Bonding from Crystal-Structure Correlations on the Enol Form of the β -Diketone Fragment. *J. Am. Chem. Soc.* **1989**, *111*, 1023–1028.
- Bertolasi, V.; Gilli, P.; Ferretti, V.; Gilli, G. Evidence for Resonance-Assisted Hydrogen Bonding. 2. Intercorrelation between Crystal Structure and Spectroscopic Parameters in Eight Intramolecularly Hydrogen-Bonded 1,3-Diaryl-1,3-Propanedione Enols. *J. Am. Chem. Soc.* **1991**, *113*, 4917–4925.
- Gilli, G.; Bertolasi, V.; Ferretti, V.; Gilli, P. Resonance-Assisted Hydrogen Bonding. III. Formation of Intermolecular Hydrogen-Bonded Chains in Crystals of β -Diketone Enols and its Relevance to Molecular Association. *Acta Crystallogr.* **1993**, *B49*, 564–576.
- Bertolasi, V.; Gilli, P.; Ferretti, V.; Gilli, G. Resonance-Assisted O–H···O Hydrogen Bonding: Its Role in the Crystalline Self-Recognition of β -Diketone Enols and its Structural and IR Characterization. *Chem.—Eur. J.* **1996**, *2*, 925–934.
- Gilli, P.; Bertolasi, V.; Ferretti, V.; Gilli, G. Evidence for Intramolecular N–H···O Resonance-Assisted Hydrogen Bonding in β -Enaminones and Related Heterodienes. A Combined Crystal-Structural, IR and NMR Spectroscopic and Quantum-Mechanical Investigation. *J. Am. Chem. Soc.* **2000**, *122*, 10405–10417.
- Gilli, P.; Bertolasi, V.; Pretto, L.; Lycka, A.; Gilli, G. The Nature of Solid-State N–H···O/O–H···N Tautomeric Competition in Resonant Systems. Intramolecular Proton Transfer in Low-Barrier Hydrogen Bonds Formed by the \cdots O=C–C=N–NH \cdots \rightleftharpoons \cdots HO–C=C–N=N \cdots Keto-hydrazone–Azoenol System. A Variable-Temperature X-Ray Crystallographic and DFT Computational Study. *J. Am. Chem. Soc.* **2002**, *124*, 13554–13567.
- Gilli, P.; Bertolasi, V.; Pretto, L.; Antonov, L.; Gilli, G. Variable-Temperature X-Ray Crystallographic and DFT Computational Study of the N–H···O/N \cdots H–O Tautomeric Competition in 1-(Arylazo)-2-Naphthols. Outline of a Transition-State Hydrogen-Bond Theory. *J. Am. Chem. Soc.* **2005**, *127*, 4943–4953.
- Gilli, P.; Bertolasi, V.; Pretto, L.; Gilli, G. Outline of a Transition-State Hydrogen-Bond Theory. *J. Mol. Struct.* **2006**, *790*, 40–49.
- Cookson, R. F. Determination of Acidity Constants. *Chem. Rev.* **1974**, *74*, 5–28.
- Smith, M. B.; March, J. *March's Advanced Organic Chemistry*, 5th ed.; Wiley: New York, 2001; Chapter 8, pp 327–362.
- Maskill, H. *The Physical Basis of Organic Chemistry*; Oxford University Press: Oxford, U.K., 1985; Chapter 5, pp 156–215.
- Lide, D. R.; Frederikse, H. P. R., Eds. *CRC Handbook of Chemistry and Physics*, 75th ed.; CRC Press: Boca Raton, FL, 1994; pp 8-43–55.
- Martell, A. E.; Smith, R. M.; Motekaitis, R. J. *NIST Critically Selected Stability Constants of Metal Complexes*, NIST Standard Reference Database Number 46, Version 8.0; NIST: Gaithersburg, MD, May 2004.
- Allen, F. H. The Cambridge Structural Database: A Quarter of a Million Crystal Structures and Rising. *Acta Crystallogr.* **2002**, *B58*, 380–388.
- Inorganic Crystal Structure Database*. Version 2006-2. FIZ-Karlsruhe, Germany, and NIST, USA.
- Meot-Ner (Mautner), M.; Lias, S. G. Thermochemistry of Cluster Ion Data. In *NIST Chemistry WebBook*; Linstrom, P. J., Mallard, W. G., Eds.; NIST Standard Reference Database Number 69; NIST: Gaithersburg, MD, June 2005, <http://webbook.nist.gov/chemistry/>.
- Bartmess, J. E. Negative Ion Energetics Data. In *NIST Chemistry WebBook*; Linstrom, P. J., Mallard, W. G., Eds.; NIST Standard Reference Database Number 69; NIST: Gaithersburg, MD, June 2005, <http://webbook.nist.gov/chemistry/>.
- Gilli, P.; Pretto, L.; Gilli, G. PA/pK_a Equalization and the Prediction of the Hydrogen-Bond Strength: A Synergism of Classical Thermodynamics and Structural Crystallography. *J. Mol. Struct.* **2007**, *844–845*, 328–339.
- Latimer, W. M.; Rodebush, W. H. Polarity and Ionization from the Standpoint of the Lewis Theory of Valence. *J. Am. Chem. Soc.* **1920**, *42*, 1419–1433.
- Vinogradov, S. N.; Linnel, R. H. *Hydrogen Bonding*; Van Nostrand Reinhold: New York, 1971; Chapter 1, pp 1–22.
- Jeffrey, G. A.; Saenger, W. *Hydrogen Bonding in Biological Structures*; Springer-Verlag: Berlin, Germany, 1991, p 36.
- Lippincott, E. R.; Schroeder, R. One-Dimensional Model of the Hydrogen Bond. *J. Chem. Phys.* **1955**, *23*, 1099–1106.
- Schroeder, R.; Lippincott, E. R. Potential Function Model of Hydrogen Bonds. II. *J. Phys. Chem.* **1957**, *61*, 921–928.
- Pedireddi, V. R.; Desiraju, G. R. A Crystallographic Scale of Carbon Acidity. *J. Chem. Soc., Chem. Commun.* **1992**, 988–990.
- Bock, H.; Dienelt, R.; Schodel, H.; Havlas, Z. The C–H···O Hydrogen-Bond Adduct of Two Trinitromethanes to Dioxane. *J. Chem. Soc., Chem. Commun.* **1993**, 1792–1793.
- Johnson, S. L.; Rumon, K. A. Infrared Spectra of Solid 1:1 Pyridine–Benzoic Acid Complexes; The Nature of the Hydrogen Bond as a Function of the Acid-Base Levels in the Complex. *J. Phys. Chem.* **1965**, *69*, 74–86.

- 48 Sobczyk, L. X-ray Diffraction, IR, UV, and NMR Studies on Proton-Transfer Equilibrating Phenol-N-Base Systems. *Ber. Bunsen-Ges. Phys. Chem.* **1998**, *102*, 377–383.
- 49 Huyskens, P.; Sobczyk, L.; Majerz, I. On a Hard/Soft Hydrogen Bond Interaction. *J. Mol. Struct.* **2002**, *615*, 61–72.
- 50 Before computing the $d'_{N\cdots O} = d_{N-H} + d_{H-O}$ distances, the N–H and O–H bond lengths were renormalized at the respective neutron distances of 1.009 and 0.97 Å whenever shorter than these values.
- 51 Gilli, G; Gilli, P. *The Nature of the Hydrogen Bond. Outline of a Comprehensive Hydrogen Bond Theory*, Oxford University Press: Oxford, U.K., 2009.